

Bound-State Beta Decay of $^{205}\text{Tl}^{81+}$ Ions and the LOREX Project

R. S. Sidhu,^{1,2,3,*} G. Leckenby,^{4,5} R. J. Chen,^{2,3,6,†} R. Mancino,^{7,2,‡} T. Neff,² Yu. A. Litvinov,^{2,8} G. Martínez-Pinedo,^{2,7,8} G. Amthauer,⁹ M. Bai,² K. Blaum,³ B. Boev,¹⁰ F. Bosch,^{2,§} C. Brandau,² V. Cvetković,¹¹ T. Dickel,^{2,12} I. Dillmann,^{4,13} D. Dmytriiev,² T. Faestermann,¹⁴ O. Forstner,² B. Franczak,² H. Geissel,^{2,12,§} R. Gernhäuser,¹⁴ J. Glorius,² C. J. Griffin,⁴ A. Gumberidze,² E. Haettner,² P.-M. Hillenbrand,^{2,15} P. Kienle,^{14,§} W. Korten,¹⁶ Ch. Kozhuharov,² N. Kuzminchuk,² K. Langanke,² S. Litvinov,² E. Menz,² T. Morgenroth,² C. Nociforo,² F. Nolden,^{2,§} M. K. Pavičević,⁹ N. Petridis,² U. Popp,² S. Purushothaman,² R. Reifarth,¹⁷ M. S. Sanjari,² C. Scheidenberger,^{2,12,18} U. Spillmann,² M. Steck,² Th. Stöhlker,² Y. K. Tanaka,¹⁹ M. Trassinelli,²⁰ S. Trotsenko,² L. Varga,^{14,2} M. Wang,⁶ H. Weick,² P. J. Woods,¹ T. Yamaguchi,²¹ Y. H. Zhang,⁶ J. Zhao,² and K. Zuber²²

(E121 and LOREX Collaborations)

¹*School of Physics and Astronomy, The University of Edinburgh, EH9 3FD Edinburgh, United Kingdom*

²*GSI Helmholtzzentrum für Schwerionenforschung, Planckstraße 1, 64291 Darmstadt, Germany*

³*Max-Planck-Institut für Kernphysik, 69117 Heidelberg, Germany*

⁴*TRIUMF, Vancouver, British Columbia V6T 2A3, Canada*

⁵*Department of Physics and Astronomy, University of British Columbia, Vancouver, BC V6T 1Z1, Canada*

⁶*Institute of Modern Physics, Chinese Academy of Sciences, 730000 Lanzhou, People's Republic of China*

⁷*Institut für Kernphysik (Theoriezentrum), Fachbereich Physik,*

Technische Universität Darmstadt, Schlossgartenstraße 2, 64289 Darmstadt, Germany

⁸*Helmholtz Forschungsakademie Hessen für FAIR (HFHF),*

GSI Helmholtzzentrum für Schwerionenforschung, Planckstraße 1, 64291 Darmstadt, Germany

⁹*Department of Chemistry and Physics of Materials,*

University of Salzburg, Jakob-Haringer-Strasse 2a, 5020 Salzburg, Austria

¹⁰*University of Štip, Faculty of Mining and Geology, Goce Delčev 89, 92000 Štip, North Macedonia*

¹¹*University of Belgrade, Faculty of Mining and Geology, Dušina 7, 11000 Belgrade, Serbia*

¹²*II. Physikalisches Institut, Justus-Liebig-Universität Gießen, 35392 Gießen, Germany*

¹³*Department of Physics and Astronomy, University of Victoria, Victoria, British Columbia V8P 5C2, Canada*

¹⁴*Physik Department, Technische Universität München, D-85748 Garching, Germany*

¹⁵*I. Physikalisches Institut, Justus-Liebig-Universität Gießen, 35392 Gießen, Germany*

¹⁶*IRFU, CEA, Université Paris-Saclay, Gif-sur-Yvette, 91191, France*

¹⁷*J.W. Goethe Universität, 60438 Frankfurt, Germany*

¹⁸*Helmholtz Research Academy Hesse for FAIR (HFHF),*

GSI Helmholtz Center for Heavy Ion Research, Campus Gießen, 35392 Gießen, Germany

¹⁹*High Energy Nuclear Physics Laboratory, RIKEN, 2-1 Hirosawa, Wako, Saitama 351-0198, Japan*

²⁰*Institut des NanoSciences de Paris, CNRS, Sorbonne Université, Paris, France*

²¹*Saitama University, Saitama 338-8570, Japan*

²²*Institut für Kern- und Teilchenphysik, Technische Universität Dresden, Zellescher Weg 19, 01062 Dresden, Germany*

(Dated: January 13, 2025)

Stable ^{205}Tl ions have the lowest known energy threshold for capturing electron neutrinos (ν_e) of $E_{\nu_e} \geq 50.6$ keV. The Lorandite Experiment (LOREX), proposed in the 1980s, aims at obtaining the longtime averaged solar neutrino flux by utilizing natural deposits of Tl-bearing lorandite ores. To determine the ν_e capture cross section, it is required to know the strength of the weak transition connecting the ground state of ^{205}Tl and the 2.3 keV first excited state in ^{205}Pb . The only way to experimentally address this transition is to measure the bound-state beta decay (β_b) of fully ionized $^{205}\text{Tl}^{81+}$ ions. After three decades of meticulous preparation, the half-life of the β_b decay of $^{205}\text{Tl}^{81+}$ has been measured to be 291_{-27}^{+33} days using the Experimental Storage Ring (ESR) at GSI, Darmstadt. The longer measured half-life compared to theoretical estimates reduces the expected signal-to-noise ratio in the LOREX, thus challenging its feasibility.

Introduction—In the past 4.6 billion years [1], the Sun has produced an abundant amount of energy through nuclear fusion reactions [2]. As a result, a huge amount of electron neutrinos (ν_e) have been, and continue to be, emitted from the Sun's interior [3, 4]. The main contribution ($\sim 91\%$) comes from the proton-proton (pp) fusion reaction. Other contributions include neutrinos from weak decays of ^7Be ($\sim 7\%$), ^8B ($\sim 0.02\%$), and CNO

cycle isotopes (see Table I). The neutrino spectroscopy provides important information on the structure of our Sun and serves as a critical means to test solar models.

Accounting for most of the solar neutrinos, pp neutrinos are extremely challenging to detect on Earth owing to their low energy ($0 \leq E_{\nu_e} \leq 422$ keV). The first neutrino experiments [5–7] observed neutrino yields much lower than expected by solar models, which was termed

as the solar-neutrino problem. In 1976, Freedman *et al.* [8] studied all weak transitions and identified the ^{205}Tl - ^{205}Pb pair to have the lowest threshold energy for ν_e capture of just 50.6 keV [9]. They proposed to search for natural deposits of lorandite ores (TlAsS_2) containing ^{205}Tl (natural abundance of 70.5%) and measure the amount of created ^{205}Pb , thereby determining the solar neutrino flux, Φ_{ν_e} , averaged over the age of the ore.

The Lorandite Experiment (LOREX) [10] was conceived by Pavićević in 1983, which relied on the rich lorandite deposits discovered in the mine of Allchar (North Macedonia) [11, 12]. Although the solar-neutrino problem was solved through the discovery of neutrino oscillations [13] at the Sudbury Neutrino Observatory (SNO) [14] and the Super-Kamiokande (Super-K) [15], and the present Φ_{ν_e} value was obtained by the BOREXINO experiment [16, 17], the possibility to obtain a long-time averaged Φ_{ν_e} remains appealing, which justified the continuation of LOREX [18].

Of the various geochemical solar-neutrino experiments, such as ^{81}Br - ^{81}Kr [19], ^{98}Mo - ^{98}Tc [20], and others [21], LOREX stands as the final geochemical neutrino project [22]. LOREX combines the geological extraction and characterization of lorandite ore, its chemical purification, and an accelerator-based measurement of ^{205}Pb concentration to determine the ν_e capture cross section of ^{205}Tl . In this Letter, we report the first direct measurement of the bound-state beta decay (β_b) of fully ionized $^{205}\text{Tl}^{81+}$, which is indispensable for the determination of the ν_e capture cross section. This decay rate is also important for the astrophysical slow neutron-capture process (the *s* process), which is discussed elsewhere [23].

The capture of solar neutrinos transforms the stable ^{205}Tl atom (ground state, $I^\pi = 1/2^+$) via the (ν_e, e^-) reaction into the radionuclide ^{205}Pb , where the first excited state [$E^* = 2.3$ keV [24], $I^\pi = 1/2^-$, $T_{1/2} = 24.2(4)$ μs] is predominantly populated due to the nuclear selection rules. This state promptly decays via internal conversion to the ground state of ^{205}Pb [$I^\pi = 5/2^-$, $T_{1/2} = 17.0(9)$ million years (Myr) [25]], making the measurement of its weak decay unfeasible. The only direct method to determine the nuclear matrix element of this weak transition is currently the measurement of the bound-state beta decay of fully ionized $^{205}\text{Tl}^{81+}$ to $^{205}\text{Pb}^{81+}$ [26].

In β_b decay [27, 28], a neutron transforms into a proton, and an electron is created in a bound atomic state instead of being emitted to a continuum, and thus, a monochromatic electron antineutrino is produced in a free state.

Experiment and analysis—The measurement was performed at GSI Helmholtzzentrum für Schwerionenforschung in Darmstadt, which is presently the only facility where such measurements are possible. Since ^{205}Tl atoms are stable, a straightforward approach would be to produce the ^{205}Tl beam directly from the ion source as was done in the first β_b -decay measurements on ^{163}Dy [29] and ^{187}Re [30]. However, Tl vapors are poi-

sonous. Therefore, $^{205}\text{Tl}^{81+}$ ions had to be produced in a nuclear reaction. An enriched ^{206}Pb material was utilized. The $^{206}\text{Pb}^{67+}$ projectile beams were accelerated to an energy of 11.4 MeV/u in the linear accelerator UNILAC and then injected into the heavy-ion synchrotron SIS-18, where they were further accelerated up to an energy of 678 MeV/u. The ^{206}Pb beams were extracted with an average intensity of 10^9 particles per pulse and impinged on a 1607 mg/cm² thick ^9Be production target backed with 223 mg/cm² niobium located at the entrance of the Fragment Separator (FRS) [31]. $^{205}\text{Tl}^{81+}$ ions were produced via a single proton knockout reaction along with numerous other reaction products. The cocktail fragment beam was analyzed by the FRS. The critical contaminant fragment is the isobaric hydrogen-like (H-like) $^{205}\text{Pb}^{81+}$ ions, which are the same as the daughter ions of the β_b decay of interest. The fully ionized $^{205}\text{Tl}^{81+}$ ions were centered throughout the FRS. An aluminum degrader with a thickness of 735 mg/cm² was used in the middle focal plane of the FRS. Owing to the Z^2 dependence of the energy losses and subsequent momentum analysis, the distributions of $^{205}\text{Pb}^{81+}$ and $^{205}\text{Tl}^{81+}$ were nearly completely spatially separated at the exit of the FRS.

About 10^4 $^{205}\text{Tl}^{81+}$ ions per spill were transmitted through the FRS and injected into the Experimental Storage Ring (ESR) [32] at 400 MeV/u. The proportion of contaminant $^{205}\text{Pb}^{81+}$ ions amounted to 0.1% of the $^{205}\text{Tl}^{81+}$ intensity. The adopted production and separation scheme is analogous to the one employed in the measurement of β_b decay of $^{207}\text{Tl}^{81+}$ [33]. However, the larger dispersion in the second half of the FRS used in this experiment enabled us to reduce the contamination by about an order of magnitude.

According to theoretical predictions, the half-life of $^{205}\text{Tl}^{81+}$ could have been as long as 1 yr [34]. Therefore, to achieve higher statistics, accumulation of $^{205}\text{Tl}^{81+}$ ions was necessary. The storage acceptance of the ESR is $\Delta B\rho/B\rho \sim \pm 1.5\%$. Fresh fragment beams were injected on an outer orbit of the ESR, where they were stochastically precooled [35]. The cooled beam was then shifted by applying a radio-frequency pulse to an inner orbit of the ESR forming a stack. This procedure was repeated up to several hundred cycles, where each newly injected beam was added to the stack. The beam was continuously cooled by an electron cooler [36, 37] (electron current $I_e = 200$ mA). Once the desired intensity was achieved [$N_{\text{Tl}}(0) \approx 1\text{--}2 \times 10^6$], stochastic cooling was switched off and the stacked beam was shifted from the inner orbit to the central orbit by ramping the dipole magnets. To allow $^{205}\text{Tl}^{81+}$ to decay, we let the beam circulate in the ultrahigh vacuum of the ESR ($\approx 10^{-10}$ mbar) for different storage times, ranging from 0 to 10 hr, while the current of the electron cooler was reduced to $I_e = 20$ mA to minimize the recombination rate with electrons.

During the storage time, some of the $^{205}\text{Tl}^{81+}$ ions de-

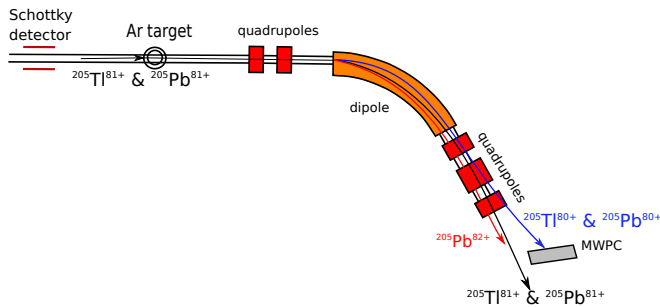


FIG. 1. Schematic of the experimental setup at the ESR from the gas jet target to the next dipole magnet. The β_b -decayed $^{205}\text{Pb}^{81+}$ daughter ions were stripped to the $q = 82+$ state, where they followed a different orbit to the main beam within the acceptance of the ring. Ions with $q = 80+$ were deflected and counted by a MWPC [43]. Both, the $^{205}\text{Tl}^{81+}$ and $^{205}\text{Pb}^{82+}$ ions were counted by a non destructive 245 MHz resonant Schottky detector [44–46].

cayed by β_b decay to H-like $^{205}\text{Pb}^{81+}$ ions with the electron created in the K shell. Because of a small $Q_{\beta_b}(K)$ value of only 31.1(5) keV [9, 25, 38], the two beams were indistinguishable by detectors in the ESR. To reveal the β_b -daughter ions at the end of each storage time, an argon (Ar) gas jet target [39, 40] with a density $\sim (2-4) \times 10^{12}$ atoms/cm² was switched on for a time interval of 10 min. As a result, the electron from $^{205}\text{Pb}^{81+}$ ions was stripped off, transforming H-like $^{205}\text{Pb}^{81+}$ ions to the fully ionized $^{205}\text{Pb}^{82+}$ ions. Thereby, the mass to charge (m/q) ratio was altered and $^{205}\text{Pb}^{82+}$ ions jumped to an inner orbit of the ring (as shown in Fig. 1). After the application of the gas target, the ions were electron cooled for 100 s and then counted for a further 40 s, see Fig. 2.

The number of β_b -daughter ions $N_{\text{Pb}}(t_s)$ grows in proportion to the storage time t_s provided that t_s is small with respect to the half-life. For that case, $N_{\text{Pb}}(t_s)$ is given to a good approximation by the relation [29, 41]

$$\frac{N_{\text{Pb}}(t_s)}{N_{\text{Tl}}(t_s)} = \frac{\lambda_b}{\gamma} t_s \left[1 + \frac{1}{2} (\lambda_{\text{Tl}}^{\text{cc}} - \lambda_{\text{Pb}}^{\text{cc}}) t_s + \dots \right] + \frac{N_{\text{Pb}}(0)}{N_{\text{Tl}}(0)} e^{(\lambda_{\text{Tl}}^{\text{cc}} - \lambda_{\text{Pb}}^{\text{cc}}) t_s}, \quad (1)$$

where $N_{\text{Tl}}(t_s)$ and $N_{\text{Pb}}(t_s)$ are, respectively, the numbers of $^{205}\text{Tl}^{81+}$ and $^{205}\text{Pb}^{81+}$ ions at time, t_s , the end of the storage, with further details on their determination provided in [42]. The ratio $N_{\text{Pb}}(0)/N_{\text{Tl}}(0)$ is the initial contamination. The detection and identification of stored ions was done with a non destructive 245 MHz Schottky resonator [44–46], where the Fourier transformed noise from the detector reveals revolution frequencies and intensities of all individual ionic species [47, 48]. The Lorentz factor was $\gamma = 1.429(1)$. The rates $\lambda_{\text{Tl}}^{\text{cc}}$ and $\lambda_{\text{Pb}}^{\text{cc}}$ account for storage losses of $^{205}\text{Tl}^{81+}$ and $^{205}\text{Pb}^{81+}$ ions, respectively, due to the atomic charge changing (cc)

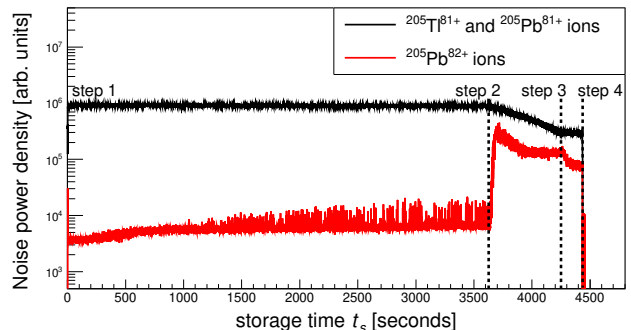


FIG. 2. Intensities of $q = 81+$ and $q = 82+$ ions during an example 1 hr storage measurement. The storage time (step 1 \rightarrow step 2), gas jet operation (step 2 \rightarrow step 3), cooling (step 3 \rightarrow step 4), and detection (step 4).

processes in the ESR. $\lambda_{\text{Tl}}^{\text{cc}} = 4.34(6) \times 10^{-5} \text{ s}^{-1}$ was measured with $^{205}\text{Tl}^{81+}$ beam. Theoretical rates of radiative recombination (RR) [49] were used to determine the difference $\lambda_{\text{Tl}}^{\text{cc}} - \lambda_{\text{Pb}}^{\text{cc}} = \lambda_{\text{Tl}}^{\text{cc}} (1 - \text{RR}_{\text{Pb}^{81+}} / \text{RR}_{\text{Tl}^{81+}}) = 3.47(5)_{\text{stat}}(87)_{\text{syst}} \times 10^{-6} \text{ s}^{-1}$.

H-like $^{205}\text{Pb}^{81+}$ ions may capture an electron from the gas jet atoms and leave the acceptance of the ESR. Thus, the number of $^{205}\text{Pb}^{82+}$ ions detected on the inner orbit needs to be corrected by the ratio $(\sigma_{\text{I,Pb}} + \sigma_{\text{C,Pb}}) / \sigma_{\text{I,Pb}}$ [29], where $\sigma_{\text{I,Pb}}$ and $\sigma_{\text{C,Pb}}$ are the ionization and capture cross sections, respectively. The ratio $(\sigma_{\text{I,Pb}} + \sigma_{\text{C,Pb}}) / \sigma_{\text{I,Pb}} = 1.425(3)_{\text{stat}}(13)_{\text{syst}}$ was obtained with a $^{206}\text{Pb}^{81+}$ beam [41]. $^{206}\text{Pb}^{80+}$ ions that captured an electron in the gas jet target were counted by a multi-wire proportional chamber (MWPC) [43] placed outside the ring vacuum behind a 25 μm stainless foil (see Fig. 1), while the total number of ions was monitored by a direct current current transformer [50].

A Monte Carlo error propagation method was used to consistently handle the applied corrections. In particular, the variation in the initial contamination of $^{205}\text{Pb}^{81+}$ ions was estimated from the data itself. To estimate the contamination variation, the χ^2 distribution was sampled for each Monte Carlo run, and then a value for the variation was determined [42]. Subsequently, the dataset was fitted to Eq. (1), see Fig. 3, and the median β_b -decay rate in the ion rest frame was determined to be $\lambda_b = 2.76(25)_{\text{stat}}(13)_{\text{syst}} \times 10^{-8} \text{ s}^{-1}$, which corresponds to a half-life of $T_{1/2} = 291_{-27}^{+33}$ days. More details on the data analysis can be found in [41, 51].

From bound decay to neutrino capture—Because of the conservation of energy, the possible final end states of the β_b decay of ^{205}Tl can only be the ground state ^{205}Pb ($I^\pi = 5/2^-$) and the first excited state ^{205}Pb ($I^\pi = 1/2^-$). Hence, the total β_b -decay rate can be expressed as $\lambda_b = \lambda_b^{5/2^-} + \lambda_b^{1/2^-}$. From the available rate of the inverse process, i.e., the decay via electron capture of ^{205}Pb into ^{205}Tl , it is possible to determine that

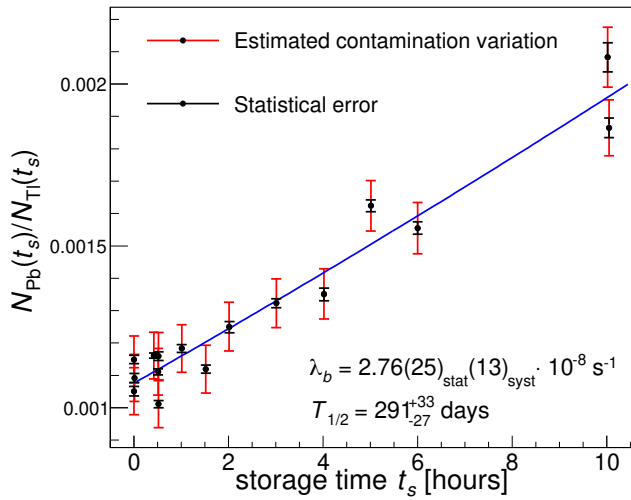


FIG. 3. $^{205}\text{Pb}^{81+}$ to $^{205}\text{Tl}^{81+}$ ratio as a function of storage time t_s . Equation (1) is used to fit (blue line) and determine the decay constant for the bound-state beta decay β_b . The error bars in black represent the statistical errors, whereas the error bars in red represent the estimated contamination variation, which accounts for the amount of $^{205}\text{Pb}^{81+}$ ions injected in the ESR from the FRS.

$\lambda_b^{5/2^-} = 1.44(8) \times 10^{-13} \text{ s}^{-1}$, and thus it has a negligible contribution.

Furthermore, considering that only the decay with the creation of an electron in the K shell of ^{205}Pb is energetically allowed, it is then possible to express the total decay rate as $\lambda_b \simeq \lambda_b^{1/2^-} = \ln(2)f_K C_K / \mathcal{K}$, where $\mathcal{K} = 2\overline{\mathcal{F}}t = 6144.5(37) \text{ s}$ is the corrected β -decay constant that includes the independent radiative correction Δ_R^V as detailed in [52], $f_K = \pi Q_{\beta_b}^2 \beta_K^2 / (2m_e^2 c^4)$ is the phase space for β_b decay, m_e is the electron mass, and β_K is the Coulomb amplitude of the K -shell electron wave function [53]. Using $\beta_K^2 = 5.567$ for H-like ^{205}Pb computed with the flexible atomic code [54], and $Q_{\beta_b} = 31.1(5) \text{ keV}$, we obtain $f_K = 0.032(1)$, which together with the measured decay rate gives a value for the nuclear shape factor for β_b decay of $C_K = 7.6(8) \times 10^{-3}$, corresponding to $\log ft = \log(\mathcal{K}/C_K) = 5.91(5)$. This shape factor has also been used as a basis for the calculations of the stellar weak rates involving ^{205}Pb and ^{205}Tl in [23]. A previous theoretical study found $C_K = 0.010$ [55].

C_K contains all relevant nuclear structure information that can be expressed in terms of the usual nuclear matrix elements for first-forbidden (ff) decays using the Behrens and Bühring formalism [56]. However, while the emitted neutrino is monoenergetic in β_b decay, in the case of neutrino capture, the equivalent nuclear shape factor, $C_{1/2_1^-}(E_{\nu_e})$ for the first excited state in ^{205}Pb ($I^\pi = 1/2^-$), must be evaluated for all values of the captured neutrino energy, E_{ν_e} , as given by the solar-neutrino spectrum. This requires us to disentangle the contributions of the different nuclear matrix elements (see [42] for

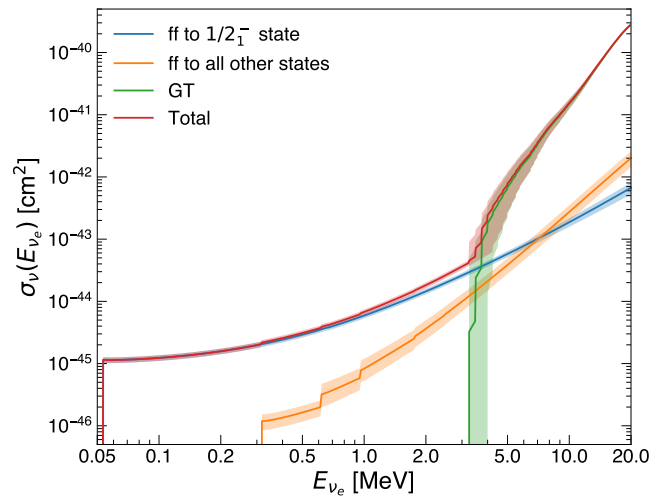


FIG. 4. Contributions to the total cross section for neutrino capture $\sigma(E_{\nu_e})$ from the ^{205}Tl ground state to ^{205}Pb , along with their relative uncertainties. Note that the total cross section is mainly determined by experimental information for all the relevant energies.

further details). For this purpose, we adopted the shell-model framework and used the NATHAN code [57] together with the Kuo-Herling hole-hole interaction [55]. Based on the shell-model calculations, we include first-forbidden contributions to the solar-neutrino capture to excited states in ^{205}Pb , beyond the ground state and the first excited state. As seen in Fig. 4, we find that first-forbidden transitions are sufficient to describe the cross section up to neutrino energies around 3 MeV. For higher neutrino energies, positive parity states in ^{205}Pb become accessible, and it is necessary to consider allowed Gamow-Teller (GT) transitions. We estimated this contribution based on charge-exchange data from the $^{205}\text{Tl}(p, n)^{205}\text{Pb}$ reaction [58].

Figure 4 shows the energy dependent cross section for neutrino capture $\sigma(E_{\nu_e})$, decomposed into the main contributions. The contribution to the cross section by the transition to $^{205}\text{Pb}(1/2_1^-)$ dominates at low neutrino energies ($E_{\nu_e} < 3 \text{ MeV}$). The cross section has been integrated over the different solar-neutrino fluxes to obtain the different contributions to the solar-neutrino capture rate, as given in Table I (see [42]). We account for neutrino oscillations using the solar-neutrino survival factors extracted from Fig. 14.3 in [59]. We also include the estimates from the work of Bahcall and Ulrich [3]. The latter have been rescaled to the values of neutrino fluxes used in this work. In parenthesis, we provide the contribution to the neutrino capture of the transition to $^{205}\text{Pb}(1/2_1^-)$. It represents the dominant contribution for all neutrino sources except for ^8B and hep neutrinos, whose rates are mainly determined by Gamow-Teller transitions.

We obtain a total neutrino capture rate of $92 \pm 10 \pm 10$ solar neutrino unit (SNU), where the first error accounts

TABLE I. Contributions of individual neutrino fluxes to the solar-neutrino capture rate on ^{205}Tl expressed in SNU. Neutrino oscillations are considered. The quoted errors account only for nuclear uncertainties. In the work of Bahcall and Ulrich [3], the capture of neutrinos from the ^{13}N , ^{15}O , and pep fluxes are considered in the total sum but not provided individually. In parentheses, the contribution to the neutrino capture of the transition to $^{205}\text{Pb}(1/2_1^-)$ is given.

Flux	Present Letter	Ref. [3]
pp	64 ± 7 (63 ± 7)	98
^7Be	14 ± 2 (12 ± 1)	19
^{13}N	0.85 ± 0.11 (0.74 ± 0.05)	-
^{15}O	0.95 ± 0.11 (0.80 ± 0.11)	-
^{17}F	0.021 ± 0.002 (0.018 ± 0.002)	-
pep	0.69 ± 0.09 (0.56 ± 0.04)	-
^8B	11 ± 2 (0.18 ± 0.02)	13
hep	$0.26^{+0.06}_{-0.03}$ (0.0019 ± 0.0003)	-
Total	92 ± 10 (77 ± 8)	135

for nuclear uncertainties and the second for the uncertainties in the neutrino survival factors. We notice that the capture cross section for pp and ^7Be neutrinos is significantly lower than the one of Bahcall and Ulrich. Lacking a measurement for the shape factor, Bahcall and Ulrich assumed a $\log ft = 5.7$ value for the first-forbidden transition to $^{205}\text{Pb}(1/2_1^-)$ from systematics. Our total neutrino capture rate is significantly higher than the one reported in [60] (62.2 ± 8.6 SNU). This is most likely due to their neglect of Gamow-Teller contributions and an underestimation of the pp -neutrino rate. Further details on the individual contributions of the different neutrino fluxes can be found in [42].

LOREX implications.—The goal of the LOREX project is to determine the longtime average of the solar neutrino flux Φ_ν via the neutrino capture reaction. The average neutrino flux over the exposure time a , which represents the age of lorandite since its mineralization, is estimated using the activation equation [11]: $\Phi_\nu = N^{-1}(T - B)(\sigma\epsilon)^{-1}\lambda[1 - \exp(-\lambda a)]^{-1}$, where N is the total number of ^{205}Tl atoms, T is the total number of ^{205}Pb atoms, B is the background-induced number of ^{205}Pb atoms (mainly produced by cosmic muons and natural radioactivity [11, 61]), σ denotes the neutrino capture cross section, ϵ represents the overall detection efficiency, and λ is the decay constant of ^{205}Pb . Considering the total neutrino capture rate of $92 \pm 10 \pm 10$ SNU determined here, the geological age of $a = 4.31(2)$ Myr [62], the electron capture probability λ of ^{205}Pb back to ^{205}Tl as $\lambda = 4.01(16) \times 10^{-8} \text{ yr}^{-1}$ [25], the molar mass M of lorandite = 343 g/mol [12], and the number of ^{205}Tl atoms

to be $1.25 \times 10^{21}(2.5 \times 10^{19})$ atoms/g of lorandite [61], we expect the time-integrated number of solar-neutrino induced ^{205}Pb atoms ($T - B$) to be 14(4) atoms/g of lorandite. This obtained value agrees within 1σ with the value quoted in [12], i.e., 22(7) ^{205}Pb atoms/g of lorandite, where a theoretical value of 146 SNU was used for the neutrino capture rate.

Presently, a total of 405.5 g of pure lorandite crystals, with a purity $> 99\%$, have been extracted from 10.5 tons of raw ore body of Crven Dol Allchar deposit. These lorandite samples are stored in a shallow underground Felsenkeller laboratory in Dresden to ensure minimal production of background-induced ^{205}Pb atoms [41]. The next significant challenge for the LOREX project is to extract the total number of Pb atoms (T) from the collected lorandite minerals. For this purpose, dedicated accelerator-based experiments are being discussed [11, 26, 61]. Additionally, it is crucial to subtract the background-induced ^{205}Pb atoms (B) which depend on factors such as the erosion rate and paleo depth of the lorandite site from where the samples are collected and can be calculated as a function of the depth of the lorandite location [61].

Conclusions—In conclusion, the measurement of the half-life of the bound-state beta decay of fully ionized $^{205}\text{Tl}^{81+}$ ions has been successfully accomplished. This experiment was one of the main motivations for the construction of the SIS-FRS-ESR facilities at GSI [63]. After 30 years since its proposal, continuous advancements in accelerator technologies, beam manipulation techniques, and detector performances have finally led to the realization of this measurement. The measured β_b -decay half-life is significantly longer, 291^{+33}_{-27} days, than previous theoretical estimates based on systematics: 122 days [64] and 52.43 days [65]. By using the new estimated rate, the solar-neutrino capture cross section has been calculated, resulting in a correspondingly lower value than previously anticipated. This has severe consequences on the geochemical neutrino experiment LOREX, which aims to determine the averaged solar neutrino flux over the last 4.31(2) Myr. Taking the estimated concentration of 14(4) solar neutrino induced ^{205}Pb atoms/g, a total of about 5677(1622) ^{205}Pb atoms are expected in the entire available lorandite sample of about 405.5 g, which corresponds to a signal-to-background ratio of only 3.5σ (assuming detection efficiency of 100%). Overall, this makes any statistically significant determination of ^{205}Pb concentration due to solar neutrinos highly unlikely. The sensitivity might be boosted by collecting significantly larger lorandite samples, preferably at higher paleo depths to reduce cosmic and geology related systematic uncertainties [11, 12, 61].

Acknowledgments—The results presented here are based on the experiment G-17-E121, which was performed at the FRS-ESR facilities at the GSI Helmholtzzentrum für Schwerionenforschung, Darmstadt

(Germany) in the framework of FAIR Phase-0. Fruitful discussions and support from U. Battino, D. Bemmerer, S. Cristallo, B. S. Gao, R. Grisenti, S. Haggmann, W. F. Henning, A. Karakas, T. Kaur, O. Klepper, W. Kutschera, M. Lestinsky, M. Lugaro, B. Meyer, A. Ozawa, V. Pejović, M. Pignatari, D. Schneider, T. Suzuki, B. Szányi, K. Takahashi, S. Yu. Torilov, X. L. Tu, D. Vescovi, P. M. Walker, E. Wiedner, N. Winckler, A. Yagüe Lopéz, and X. H. Zhou are greatly acknowledged. The authors thank the GSI accelerator team for providing excellent technical support, in particular, to R. Heß, C. Peschke, and J. Rofsbach from the GSI beam cooling group. We thank the Extreme Matter Institute EMMI at GSI, Darmstadt, for support in the framework of an EMMI Rapid Reaction Task Force meeting. This work was supported by the European Research Council (ERC) under the EU's Horizon 2020 research and innovation program (Grant Agreement Nos. 682841 "ASTRUM" and 654002 "ENSAR2"); the Natural Sciences and Engineering Research Council of Canada (NSERC) (NSERC Discovery Grant No. SAPIN-2019-00030); the Excellence Cluster ORIGINS from the German Research Foundation DFG (Excellence Strategy EXC-2094-390783311); the Science and Technology Facilities Council (STFC) (Grant No. ST/P004008/1); and the Sumitomo Foundation, Mitsubishi Foundation, JSPS KAKENHI Nos. 26287036, 17H01123, 23KK0055. R.M. and G.M.P. acknowledge support by the Deutsche Forschungsgemeinschaft (DFG, German Research Foundation)—Project-ID 279384907 - SFB 1245. Y.H.Z. acknowledges the support from EMMI at GSI in the form of an EMMI Visiting Professorship. R.M. acknowledges the support provided by Grant No. 23-06439S of the Czech Science Foundation.

The authors declare that they have no known competing financial interests or personal relationships that could have appeared to influence the work reported in this Letter.

* ragan.sidhu@ed.ac.uk

† r.chen@gsi.de

‡ riccardo.mancino@matfyz.cuni.cz; Present address: Faculty of Mathematics and Physics, Charles University, Prague, Czech Republic

§ Deceased

- [1] A. Bonanno, H. Schlattl, and L. Paternò, *Astronomy & Astrophysics* **390**, 1115 (2002).
- [2] E. G. Adelberger, A. García, R. G. H. Robertson, K. A. Snover, A. B. Balantekin, K. Heeger, M. J. Ramsey-Musolf, D. Bemmerer, A. Junghans, C. A. Bertulani, *et al.*, *Rev. Mod. Phys.* **83**, 195 (2011).
- [3] J. N. Bahcall and R. K. Ulrich, *Rev. Mod. Phys.* **60**, 297 (1988).
- [4] W. Haxton, R. Hamish Robertson, and A. M. Serenelli, *Annual Review of Astronomy and Astrophysics* **51**, 21 (2013).
- [5] T. A. Kirsten, *Rev. Mod. Phys.* **71**, 1213 (1999).
- [6] J. Abdurashitov, E. Faizov, V. Gavrin, A. Gusev, A. Kalikhov, T. Knodel, I. Knyshenko, V. Kornoukhov, I. Mirmov, A. Pshukov, *et al.*, *Physics Letters B* **328**, 234 (1994).
- [7] P. Anselmann, W. Hampel, G. Heusser, J. Kiko, T. Kirsten, E. Pernicka, R. Plaga, U. Rönn, M. Sann, C. Schlosser, *et al.*, *Physics Letters B* **285**, 376 (1992).
- [8] M. S. Freedman, C. M. Stevens, E. P. Horwitz, L. H. Fuchs, J. L. Lerner, L. S. Goodman, W. J. Childs, and J. Hessler, *Science* **193**, 1117 (1976).
- [9] M. Wang, W. Huang, F. Kondev, G. Audi, and S. Naimi, *Chinese Physics C* **45**, 030003 (2021).
- [10] M. K. Pavičević, Lorandite from Allchar – A low energy solar neutrino dosimeter, *Nuclear Instruments and Methods in Physics Research Section A: Accelerators, Spectrometers, Detectors and Associated Equipment* **271**, 287 (1988).
- [11] M. Pavičević, F. Bosch, G. Amthauer, I. Aničin, B. Boev, W. Brüchle, Z. Djurcic, T. Faestermann, W. Henning, R. Jelenković, and V. Pejović, *Nuclear Instruments and Methods in Physics Research Section A: Accelerators, Spectrometers, Detectors and Associated Equipment* **621**, 278 (2010).
- [12] M. K. Pavičević, G. Amthauer, V. Cvetković, B. Boev, V. Pejović, W. F. Henning, F. Bosch, Y. A. Litvinov, and R. Wagner, *Nuclear Instruments and Methods in Physics Research Section A: Accelerators, Spectrometers, Detectors and Associated Equipment* **895**, 62 (2018).
- [13] B. Pontecorvo, *Zh. Eksp. Teor. Fiz.* **53**, 1717 (1967).
- [14] Q. R. Ahmad, R. C. Allen, T. C. Andersen, J. D. Anglin, J. C. Barton, E. W. Beier, M. Bercovitch, J. Bigu, S. D. Biller, R. A. Black, *et al.* (SNO Collaboration), *Phys. Rev. Lett.* **89**, 011301 (2002).
- [15] Y. Suzuki, *The European Physical Journal C* **79**, 1 (2019).
- [16] G. Bellini, J. Benziger, D. Bick, G. Bonfini, D. Bravo, B. Caccianiga, L. Cadonati, F. Calaprice, A. Caminata, P. Cavalcante, *et al.* (BOREXINO), *Nature* **512**, 383 (2014).
- [17] M. Agostini, K. Altenmüller, S. Appel, V. Atroshchenko, Z. Bagdasarian, D. Basilico, G. Bellini, J. Benziger, D. Bick, G. Bonfini, *et al.* (BOREXINO), *Nature* **562**, 505 (2018).
- [18] EMMI Rapid Reaction Task Force (RRTF) - LORandite Experiment (LOREX).
- [19] V. Kuzminov, A. Pomansky, and V. Chihladze, *Nuclear Instruments and Methods in Physics Research Section A: Accelerators, Spectrometers, Detectors and Associated Equipment* **271**, 257 (1988).
- [20] J. N. Bahcall, *Physical Review D* **38**, 2006 (1988).
- [21] R. L. Hahn, in *Journal of Physics: Conference Series*, Vol. 136 (IOP Publishing, 2008) p. 022003.
- [22] T. A. Kirsten, edited by K. Winter (Cambridge University Press, Cambridge, 1991).
- [23] G. Leckenby, R. S. Sidhu, R. J. Chen, R. Mancino, *et al.*, *Nature* **635**, 321 (2024).
- [24] F. Kondev, *Nuclear Data Sheets* **166**, 1 (2020).
- [25] F. Kondev, M. Wang, W. Huang, S. Naimi, and G. Audi, *Chinese Physics C* **45**, 030001 (2021).
- [26] Y. A. Litvinov *et al.*, E121 experiment proposal, GPAC-GSI (2017).
- [27] R. Daudel, M. Jean, and M. Lecoïn, *J. Phys. Radium* **8**,

- 238 (1947).
- [28] J. N. Bahcall, *Phys. Rev.* **124**, 495 (1961).
- [29] M. Jung, F. Bosch, K. Beckert, H. Eickhoff, H. Folger, B. Franzke, A. Gruber, P. Kienle, O. Klepper, W. Koenig, *et al.*, *Phys. Rev. Lett.* **69**, 2164 (1992).
- [30] F. Bosch, T. Faestermann, J. Friese, F. Heine, P. Kienle, E. Wefers, K. Zeitelhack, K. Beckert, B. Franzke, O. Klepper, *et al.*, *Phys. Rev. Lett.* **77**, 5190 (1996).
- [31] H. Geissel, P. Armbruster, K. H. Behr, A. Brünle, K. Burkard, M. Chen, H. Folger, B. Franczak, H. Keller, O. Klepper, *et al.*, *Nuclear Instruments and Methods in Physics Research Section B: Beam Interactions with Materials and Atoms* **70**, 286 (1992).
- [32] B. Franzke, *Nuclear Instruments and Methods in Physics Research Section B: Beam Interactions with Materials and Atoms* **24-25**, 18 (1987).
- [33] T. Ohtsubo, F. Bosch, H. Geissel, L. Maier, C. Scheidenberger, F. Attallah, K. Beckert, P. Beller, D. Boutin, T. Faestermann, *et al.*, *Phys. Rev. Lett.* **95**, 052501 (2005).
- [34] K. Takahashi and K. Yokoi, *Nuclear Physics A* **404**, 578 (1983).
- [35] F. Nolden, D. Böhne, W. Bourgeois, B. Franzke, M. Steck, and A. Schwinn, *Nuclear Physics A* **626**, 491 (1997).
- [36] G. Budker, N. Dikanskij, D. Pestrikov, I. Meshkov, V. Kudelainen, B. Sukhina, V. Parkhomchuk, and A. Skrinsky, *Part. Accel.* **7**, 197 (1976).
- [37] M. Steck, P. Beller, K. Beckert, B. Franzke, and F. Nolden, *Nuclear Instruments and Methods in Physics Research Section A: Accelerators, Spectrometers, Detectors and Associated Equipment* **532**, 357 (2004).
- [38] A. Kramida, Y. Ralchenko, and J. Reader, *National Institute of Standards and Technology, Gaithersburg, MD* (2023).
- [39] N. Petridis, R. Grisenti, Y. A. Litvinov, and T. Stöhlker, *Physica Scripta* **2015**, 014051 (2015).
- [40] N. Petridis, *PhD Thesis, Johann Wolfgang Goethe-Universität* (2014).
- [41] R. S. Sidhu, *PhD Thesis, Ruprecht-Karls-Universität* (2021).
- [42] R. S. Sidhu, G. Leckenby, R. J. Chen, R. Mancino, T. Neff, *et al.*, (2024), Supplemental Material for more details, which includes Refs. [29, 30, 41, 51–53, 55–59, 66–74].
- [43] O. Klepper and C. Kozhuharov, *Nuclear Instruments and Methods in Physics Research Section B: Beam Interactions with Materials and Atoms* **204**, 553 (2003).
- [44] F. Nolden, P. Hülsmann, Y. Litvinov, P. Moritz, C. Peschke, P. Petri, M. Sanjari, M. Steck, H. Weick, J. Wu, Y. Zang, S. Zhang, and T. Zhao, *Nuclear Instruments and Methods in Physics Research Section A: Accelerators, Spectrometers, Detectors and Associated Equipment* **659**, 69 (2011).
- [45] M. S. Sanjari, P. Hülsmann, F. Nolden, A. Schempp, J. X. Wu, D. Atanasov, F. Bosch, C. Kozhuharov, Y. A. Litvinov, P. Moritz, C. Peschke, P. Petri, D. Shubina, M. Steck, H. Weick, N. Winckler, Y. D. Zang, and T. C. Zhao, *Phys. Scr.* **2013**, 014088 (2013).
- [46] M. S. Sanjari, *PhD Thesis, Johann Wolfgang Goethe-Universität* (2013).
- [47] Y. A. Litvinov and F. Bosch, *Rep. Prog. Phys.* **74**, 016301 (2011).
- [48] M. Steck and Y. A. Litvinov, *Prog. Part. Nucl. Phys.* **115**, 103811 (2020).
- [49] M. Pajek and R. Schuch, *Phys. Rev. A* **45**, 7894 (1992).
- [50] H. Reeg and N. Schneider, *Proceedings of DIPAC 2001*, 120 (2001).
- [51] G. Leckenby, R. S. Sidhu, R. J. Chen, Y. Litvinov, J. Glorius, C. Griffin, and I. Dillmann (E121 Collaboration), *EPJ Web Conf.* **279**, 06010 (2023).
- [52] J. C. Hardy and I. S. Towner, *Phys. Rev. C* **102**, 045501 (2020).
- [53] W. Bambynek, H. Behrens, M. H. Chen, B. Crasemann, M. L. Fitzpatrick, K. W. D. Ledingham, H. Genz, M. Mutterer, and R. L. Intemann, *Rev. Mod. Phys.* **49**, 77 (1977).
- [54] M. F. Gu, *Canadian Journal of Physics* **86**, 675 (2008).
- [55] E. K. Warburton, *Phys. Rev. C* **44**, 233 (1991).
- [56] H. Behrens and W. Bühring, *Electron radial wave functions and nuclear beta decay* (Clarendon, Oxford, 1982).
- [57] E. Caurier, G. Martínez-Pinedo, F. Nowacki, A. Poves, and A. P. Zuker, *Rev. Mod. Phys.* **77**, 427 (2005).
- [58] D. Krofcheck, *PhD Thesis, Ohio State University* (1987).
- [59] S. Navas, C. Amsler, T. Gutsche, C. Hanhart, J. J. Hernández-Rey, C. Lourenço, A. Masoni, M. Mikhasenko, R. E. Mitchell, C. Patrignani, *et al.* (Particle Data Group Collaboration), *Phys. Rev. D* **110**, 030001 (2024).
- [60] J. Kostensalo, J. Suhonen, and K. Zuber, *Phys. Rev. C* **101**, 031302 (2020).
- [61] M. Pavićević, F. Bosch, G. Amthauer, I. Aničin, B. Boev, W. Brüchle, V. Cvetković, Z. Djurčić, W. Henning, R. Jelenković, *et al.*, *Advances in High Energy Physics* **2012** (2012).
- [62] F. Neubauer, M. K. Pavićević, J. Genser, R. Jelenković, B. Boev, and G. Amthauer, *Geochim. Cosmochim. Acta* **73**, 938 (2009).
- [63] P. Kienle, *Nuclear Instruments and Methods in Physics Research Section A: Accelerators, Spectrometers, Detectors and Associated Equipment* **271**, 277 (1988).
- [64] K. Takahashi, R. N. Boyd, G. J. Mathews, and K. Yokoi, *Phys. Rev. C* **36**, 1522 (1987).
- [65] S. Liu, C. Gao, and C. Xu, *Phys. Rev. C* **104**, 024304 (2021).
- [66] C. Trageser, C. Brandau, C. Kozhuharov, Y. A. Litvinov, A. Müller, F. Nolden, S. Sanjari, and T. Stöhlker, *Phys. Scr.* **2015**, 014062 (2015).
- [67] C. Trageser, *PhD Thesis, Justus-Liebig-Universität* (2018).
- [68] D. J. Millener, D. E. Alburger, E. K. Warburton, and D. H. Wilkinson, *Phys. Rev. C* **26**, 1167 (1982).
- [69] Q. Zhi, E. Caurier, J. J. Cuenca-García, K. Langanke, G. Martínez-Pinedo, and K. Sieja, *Phys. Rev. C* **87**, 025803 (2013).
- [70] R. Mancino, T. Neff, and G. Martínez-Pinedo, (to be published).
- [71] G. K. Schenter and P. Vogel, *Nucl. Sci. and Eng.* **83**, 393 (1983).
- [72] M. C. Gonzalez-Garcia, M. Maltoni, J. P. Pinheiro, and A. M. Serenelli, *J. of High Energy Phys.* **2024**, 64 (2024).
- [73] J. N. Bahcall, *Software and data for solar neutrino research* (2005).
- [74] B. Longfellow, A. T. Gallant, T. Y. Hirsh, M. T. Burkey, G. Savard, N. D. Scielzo, L. Varriano, M. Brodeur, D. P. Burdette, J. A. Clark, D. Lascar, P. Mueller, D. Ray, K. S. Sharma, A. A. Valverde, G. L. Wilson, and X. L. Yan, *Phys. Rev. C* **107**, L032801 (2023).

Supplemental Material for: Bound-State Beta Decay of $^{205}\text{Tl}^{81+}$ Ions and the LOREX Project

R. S. Sidhu,^{1,2,3,*} G. Leckenby,^{4,5} R. J. Chen,^{2,3,6,†} R. Mancino,^{7,2,‡} T. Neff,² Yu. A. Litvinov,^{2,8} G. Martínez-Pinedo,^{2,7,8} G. Amthauer,⁹ M. Bai,² K. Blaum,³ B. Boev,¹⁰ F. Bosch,^{2,§} C. Brandau,² V. Cvetković,¹¹ T. Dickel,^{2,12} I. Dillmann,^{4,13} D. Dmytriiev,² T. Faestermann,¹⁴ O. Forstner,² B. Franczak,² H. Geissel,^{2,12,§} R. Gernhäuser,¹⁴ J. Glorius,² C. J. Griffin,⁴ A. Gumberidze,² E. Haettner,² P.-M. Hillenbrand,^{2,15} P. Kienle,^{14,§} W. Korten,¹⁶ Ch. Kozhuharov,² N. Kuzminchuk,² K. Langanke,² S. Litvinov,² E. Menz,² T. Morgenroth,² C. Nociforo,² F. Nolden,^{2,§} M. K. Pavičević,⁹ N. Petridis,² U. Popp,² S. Purushothaman,² R. Reifarth,¹⁷ M. S. Sanjari,² C. Scheidenberger,^{2,12,18} U. Spillmann,² M. Steck,² Th. Stöhlker,² Y. K. Tanaka,¹⁹ M. Trassinelli,²⁰ S. Trotsenko,² L. Varga,^{14,2} M. Wang,⁶ H. Weick,² P. J. Woods,¹ T. Yamaguchi,²¹ Y. H. Zhang,⁶ J. Zhao,² and K. Zuber²²

(E121 and LOREX Collaborations)

¹School of Physics and Astronomy, The University of Edinburgh, EH9 3FD Edinburgh, United Kingdom

²GSI Helmholtzzentrum für Schwerionenforschung, Planckstraße 1, 64291 Darmstadt, Germany

³Max-Planck-Institut für Kernphysik, 69117 Heidelberg, Germany

⁴TRIUMF, Vancouver, British Columbia V6T 2A3, Canada

⁵Department of Physics and Astronomy, University of British Columbia, Vancouver, BC V6T 1Z1, Canada

⁶Institute of Modern Physics, Chinese Academy of Sciences, 730000 Lanzhou, People's Republic of China

⁷Institut für Kernphysik (Theoriezentrum), Fachbereich Physik,

Technische Universität Darmstadt, Schlossgartenstraße 2, 64289 Darmstadt, Germany

⁸Helmholtz Forschungsakademie Hessen für FAIR (HFHF),

GSI Helmholtzzentrum für Schwerionenforschung, Planckstraße 1, 64291 Darmstadt, Germany

⁹Department of Chemistry and Physics of Materials, University of Salzburg, Jakob-Haringer-Strasse 2a, 5020 Salzburg, Austria

¹⁰University of Štip, Faculty of Mining and Geology, Goce Delčev 89, 92000 Štip, North Macedonia

¹¹University of Belgrade, Faculty of Mining and Geology, Đušina 7, 11000 Belgrade, Serbia

¹²II. Physikalisches Institut, Justus-Liebig-Universität Gießen, 35392 Gießen, Germany

¹³Department of Physics and Astronomy, University of Victoria, Victoria, British Columbia V8P 5C2, Canada

¹⁴Physik Department, Technische Universität München, D-85748 Garching, Germany

¹⁵I. Physikalisches Institut, Justus-Liebig-Universität Gießen, 35392 Gießen, Germany

¹⁶IRFU, CEA, Université Paris-Saclay, Gif-sur-Yvette, 91191, France

¹⁷J.W. Goethe Universität, 60438 Frankfurt, Germany

¹⁸Helmholtz Research Academy Hesse for FAIR (HFHF),

GSI Helmholtz Center for Heavy Ion Research, Campus Gießen, 35392 Gießen, Germany

¹⁹High Energy Nuclear Physics Laboratory, RIKEN, 2-1 Hirosawa, Wako, Saitama 351-0198, Japan

²⁰Institut des NanoSciences de Paris, CNRS, Sorbonne Université, Paris, France

²¹Saitama University, Saitama 338-8570, Japan

²²Institut für Kern- und Teilchenphysik, Technische Universität Dresden, Zellescher Weg 19, 01062 Dresden, Germany

(Dated: January 13, 2025)

Determination of ion numbers—To calculate the β_b decay constant λ_b in Eq. (1) of the main paper, the number of mother $^{205}\text{Tl}^{81+}$ ($N_{\text{Tl}}(t_s)$) and β_b -daughter $^{205}\text{Pb}^{81+}$ ($N_{\text{Pb}}(t_s)$) ions needs to be measured at the end of the storage measurement, t_s . These ion numbers were determined at the end of the storage measurement, step 2 in Fig. 2 in the main paper, from the measured ion numbers at step 4 using the following equations

$$N_{\text{Tl}}(t_s) = N_{\text{Tl}}^{\text{step4}}(t_s) S_{\text{C}}(t_s) \frac{1}{e^{-\lambda_{\text{Tl}} \Delta t}}, \quad (1)$$

$$N_{\text{Pb}}(t_s) = N_{\text{Pb}}^{\text{step4}}(t_s) \frac{\sigma_{\text{I,Pb}} + \sigma_{\text{C,Pb}}}{\sigma_{\text{I,Pb}}} \frac{1}{R_{\text{C}}} \frac{1}{1 - e^{-\lambda_{\text{Pb}} \Delta t}}, \quad (2)$$

where $\Delta t = 10$ min is the time duration for which the gas jet target was turned on, and $\sigma_{\text{I,Pb}}$ and $\sigma_{\text{C,Pb}}$ are the ionization and capture cross sections for ^{205}Pb , respectively. The decay constants λ_{Tl} and λ_{Pb} were measured individually

for each storage period to account for fluctuations in target density. $S_{\text{C}}(t_s)$ accounts for a saturation effect, which was directly proportional to the beam intensity, caused by a mismatched amplifier switch in the data acquisition system [1, 2]. It has been calibrated with a low-intensity measurement and a current transformer, more details of which can be found in [3, 4]. R_{C} is the correction coefficient used to account for the resonance response of the 245 MHz Schottky detector. The R_{C} was calibrated with multiple ion species, the frequencies of which were modified when moving the beam after the accumulation was completed [3, 4].

Estimated contamination variation—The $^{205}\text{Pb}^{81+}$ ions created by one neutron knockout in the projectile fragmentation reaction in the FRS provide a significant source of contamination for the measurement of the β_b decay of $^{205}\text{Tl}^{81+}$. From Fig. 3 in the main paper, the $t_s = 0$ intercept indicates that the contamination was at the $\approx 0.11\%$ level, which was larger than the β_b signal even after 10 hrs of stor-

age. In previous β_b -decay experiments [5, 6], the authors were able to purge the β_b -daughter contaminants by turning on the gas jet target before storage, which reduced their contamination to essentially zero. After stacking reached saturation, they achieved up to 10^8 stored ions. As they were working with primary beams, losing parent ions during the purging procedure was not an issue. Whereas, we achieved $\sim 1\text{-}2 \times 10^6$ ions as we were stacking secondary beams and could not afford the loss in beam intensity.

The contaminant $^{205}\text{Pb}^{81+}$ ions from the FRS were expected to be stable across storage times and thus provided an additive offset to the observed signal that we fit as a free parameter. However, after controlling for all other sources of error, the χ^2 of our data was 302.7, which is well beyond the 95% confidence interval of [6.6, 23.7] for 14 degrees of freedom. Thus, in the absence of any other plausible explanation, we concluded that the contamination from the FRS must have varied stochastically on the 1% level. This was supported by estimates of the magnet stability throughout the FRS chain. It was challenging to get an accurate estimate of the size of the variation though, because 99.9% of contaminant $^{205}\text{Pb}^{81+}$ was blocked by the FRS slits, so the magnet variation would be affecting the tails of the straggling distribution at $> 3\sigma$. At these extremes, the tails are most likely non-Gaussian and could behave in non-linear ways.

Despite this fact, in ignorance of the exact mechanism, the most conservative choice is to model this variation as Gaussian noise by appealing to the central limit theorem. We used the χ^2 of our data to estimate the size of the error coming from contamination variation, assuming the same distribution for each storage time. In particular,

$$\chi^2 = \sum_i \frac{(\text{data}_i - \text{model}_i)^2}{\sigma_{i,\text{stat}}^2 + (\sigma_{CV} \exp[(\lambda_{\text{Tl}}^{\text{loss}} - \lambda_{\text{Pb}}^{\text{loss}})t_s])^2}, \quad (3)$$

summing over the i^{th} storage time where $\sigma_{i,\text{stat}}$ is the 1σ statistical uncertainty from all other components and σ_{CV} is the 1σ statistical uncertainty to be estimated (CV: contamination variation). Note the $\exp[(\lambda_{\text{Tl}}^{\text{loss}} - \lambda_{\text{Pb}}^{\text{loss}})t_s]$ factor accounts for the evolution of the initial contamination due to the different loss rates. To account for the fact that the χ^2 of the data is itself a statistical value, we sampled the $\chi^2(\nu = 14)$ distribution for each run of the Monte Carlo error propagation to determine the value of σ_{CV} that would be used for that Monte Carlo run. The map between the $\chi^2(\nu = 14)$ and σ_{CV} values is shown in Fig. 1. Each Monte Carlo run thus had its own unique σ_{CV} value, which was used to add variation to each data point in the Monte Carlo error propagation. This effect contributed to 69% of our total uncertainty.

Nuclear shape factors—The nuclear shape factors, C_K and $C(E_e)$, which determine the β_b decay rate and the neutrino cross section, can be expressed in terms of the appropriate nuclear matrix elements. For first-forbidden (ff) transitions, these are $w, w', x, x', u, u', z, \xi'v$, and $\xi'y$ as defined

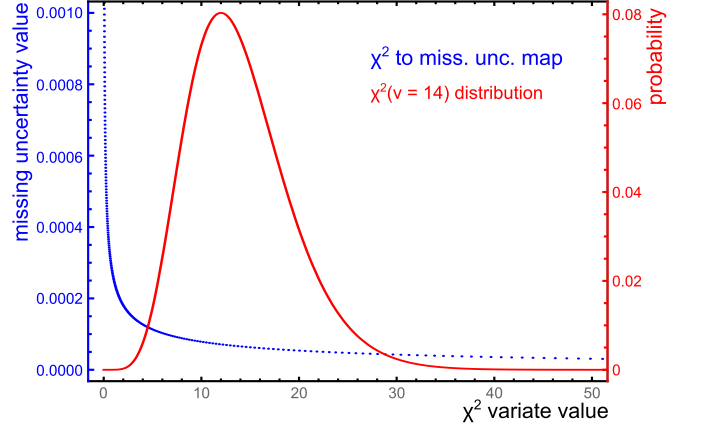


FIG. 1. The mapping of the $\chi^2(\nu = 14)$ value to the σ_{CV} value for our data set. By sampling the χ^2 distribution, we avoided the statistical invalidity of normalizing to $\chi^2 = 14$.

in [7–9].

In the case of β_b decay of fully ionized ^{205}Tl , we have [10]

$$C_K = \left[\xi w' + \xi'v + \frac{1}{3}W_0^b w - \frac{1}{3}w \right]^2 + \left[\xi(x' + u') - \xi'y + \frac{1}{3}W_0^b x + \frac{1}{3}(W_e^b - W_{\nu_e}^b)u - \frac{1}{3}(x + u) \right]^2 + \frac{1}{18}(W_{\nu_e}^b)^2(2x + u)^2 + \frac{1}{12}(W_{\nu_e}^b)^2 z^2, \quad (4)$$

where $W_e^b = 1 - I(^{205}\text{Pb}^{81+})/m_e c^2$, with the ionization energy of $^{205}\text{Pb}^{81+}$, $I(^{205}\text{Pb}^{81+}) = 101.336$ keV. $W_{\nu_e}^b$ is the energy of the emitted neutrino in units of the electron rest mass energy, $W_{\nu_e}^b = Q_{\beta_b}/(m_e c^2)$, and $W_0^b = W_e^b + W_{\nu_e}^b$. $\xi = \alpha Z \lambda_e / (2R)$ is a measure of the Coulomb energy of a uniform sphere of radius R approximating the nuclear charge distribution, where λ_e is the reduced electron Compton wavelength.

In the case of neutrino capture on neutral ^{205}Tl to a state j in ^{205}Pb , the shape factor is given by [7–9]

$$C_{j,\nu}(W_e^\nu) = k + ka W_e^\nu + \frac{kb}{W_e^\nu} + kc (W_e^\nu)^2, \quad (5)$$

where $W_e^\nu = W_{\nu_e}^\nu + (\Delta M c^2 - E_j^*) / (m_e c^2) + 1$ is the energy of the emitted electron in units of the electron rest mass energy, with $\Delta M c^2 = -50.6(5)$ keV being the difference in atomic masses between ^{205}Tl and ^{205}Pb . $W_{\nu_e}^\nu$ is the energy of the absorbed neutrino in units of the electron rest mass energy, and E_j^* is the excitation energy of the final ^{205}Pb j state. The coefficients k, ka, kb , and kc are given by

$$k = \left[\zeta_0^2 + \frac{1}{9}w^2 \right] + \left[\zeta_1^2 + \frac{1}{9}(x + u)^2 - \frac{4}{9}\gamma_1 \mu_1 u(x + u) + \frac{1}{18}(W_0^\nu)^2(2x + u)^2 - \frac{1}{18}\lambda_2(2x - u)^2 \right] + \frac{1}{12} \left[(W_0^\nu)^2 - \lambda_2 \right] z^2, \\ ka = \left[-\frac{4}{3}uY - \frac{1}{9}W_0^\nu(4x^2 + 5u^2) \right] - \left[\frac{1}{6}W_0^\nu z^2 \right], \\ kb = -\frac{2}{3}\mu_1 \gamma_1 \left\{ -[\zeta_0 w] + [\zeta_1(x + u)] \right\}, \\ kc = \left[\frac{4}{9}u^2 + \frac{1}{18}(2x + u)^2 + \frac{1}{18}\lambda_2(2x - u)^2 \right] + \frac{1}{12}(1 + \lambda_2)z^2, \quad (6)$$

with

$$\begin{aligned} V &= \xi'v + \xi w', & Y &= \xi'y - \xi(x' + u') \\ \zeta_0 &= V + \frac{1}{3}W_0^\nu w, & \zeta_1 &= Y + \frac{1}{3}W_0^\nu(u - x), \end{aligned} \quad (7)$$

where $W_0^\nu = W_e^\nu - W_{\nu_e}^\nu = (\Delta Mc^2 - E_j^*)/(m_e c^2) + 1$, $\gamma_1 = \sqrt{1 - (\alpha Z)^2}$, and μ_1 and λ_2 are Coulomb functions that account for the differences in the distortion of the electron wavefunctions with different wave numbers by the Coulomb potential of the nucleus.

For heavy nuclei like the ones considered in this work, we have $\xi \gg W_0$. In our case, $\xi = 16.3$ and $W_0^b = 0.86$. In addition, for neutrino energies $E_\nu \ll \xi m_e c^2 \approx 8$ MeV, which includes the full energy range of pp neutrinos, it is enough to consider the relativistic matrix elements $\xi'v$ and $\xi'y$, together with those terms that are multiplied by ξ in the evaluation of the shape factors for both β_b decay and neutrino capture. Under this approximation, the neutrino capture shape factor becomes energy independent and we have

$$C_K \approx C_\nu \approx [\xi'v + \xi w']^2 + [\xi'y - \xi(x' + u')]^2. \quad (8)$$

Given the fact that the solar neutrino spectrum reaches neutrino energies for which the approximation above may become invalid, we consider the full energy dependence in Eq. (5) when evaluating cross sections for first-forbidden transitions. We include first-forbidden transition to negative parity states in ^{205}Pb , based on shell-model calculations using the NATHAN code [11] together with the Kuo-Herling hole-hole interaction [12]. The matrix elements have been evaluated using the quenching factors determined in [9] that give a value of $C_K^{\text{theo}} = 8.0(24) \times 10^{-3}$ for the $^{205}\text{Tl}(1/2_1^+)$ to $^{205}\text{Pb}(1/2_1^-)$ transition. We have assigned a relative error of 30% to the shell-model value corresponding to the average root mean square difference obtained when computing the shape factor of the experimentally known first-forbidden beta decays of ^{205}Au , ^{205}Hg , ^{206}Hg , ^{206}Tl , and ^{207}Tl [9, 13]. The shell-model value agrees with the experimental result $C_K = 7.6(8) \times 10^{-3}$ measured in this work.

To fully account for the experimental data when describing the neutrino absorption to the first $1/2^-$ state in ^{205}Pb , we write the neutrino capture shape factor as

$$C_{1/2_1^-, \nu}(W_e) = C_K^{\text{exp}} + \left[C_{1/2_1^-, \nu}^{\text{theo}}(W_e) - C_K^{\text{theo}} \right], \quad (9)$$

where the second term is evaluated using the theoretical values for the matrix elements. Based on the approximation discussed above, we expect this contribution to give a very small energy dependence to the shape factor at low energies. We express the energy dependent shape factor as a function of the neutrino-energy as a Taylor expansion around the mean energy of the captured pp neutrinos of

TABLE I. Contributions of individual neutrino fluxes to the solar neutrino capture rate on ^{205}Tl expressed in SNU. These rates have to be multiplied by the neutrino oscillation survival factors. In parenthesis, the contribution to the neutrino capture of the transition to $^{205}\text{Pb}(1/2_1^-)$ are given.

Flux	Capture rate	Survival factor
pp	113 ± 12 (110 ± 12)	0.57 ± 0.09
^7Be	26 ± 3 (23 ± 2)	0.53 ± 0.05
^{13}N	1.6 ± 0.2 (1.4 ± 0.1)	0.53 ± 0.05
^{15}O	1.8 ± 0.2 (1.5 ± 0.2)	0.53 ± 0.05
^{17}F	0.039 ± 0.004 (0.034 ± 0.004)	0.53 ± 0.05
pep	1.6 ± 0.2 (1.3 ± 0.1)	0.43 ± 0.11
$^8\text{B}_{\text{ff}}$	1.2 ± 0.2 (0.55 ± 0.07)	0.32 ± 0.02
$^8\text{B}_{\text{GT}}$	34^{+7}_{-5}	0.32 ± 0.02
hep_{ff}	0.016 ± 0.003 (0.0058 ± 0.0009)	0.32 ± 0.02
hep_{GT}	$0.8^{+0.2}_{-0.1}$	0.32 ± 0.02
Total	180 ± 17 (138 ± 15)	-

$E_0 = 284$ keV as

$$\begin{aligned} C_{1/2_1^-}(E_{\nu_e}) &= 7.6(8) \times 10^{-3} + 0.14(4) \times 10^{-3} \\ &+ 0.56(17) \times 10^{-3} \left(\frac{E_{\nu_e} - E_0}{1 \text{ MeV}} \right) \\ &+ 0.027(8) \times 10^{-3} \left(\frac{E_{\nu_e} - E_0}{1 \text{ MeV}} \right)^2. \end{aligned} \quad (10)$$

The above expression reproduces the energy dependent shape factor for all energies relevant to the solar-neutrino spectrum.

In addition to the first-forbidden contribution, we also consider allowed Gamow-Teller (GT) transitions based on the charge-exchange data from the $^{205}\text{Tl}(p,n)^{205}\text{Pb}$ reaction [14]. In this case, the shape factor is energy independent and is related to the Gamow-Teller matrix element as

$$C_{\text{GT}, \nu} = B(\text{GT}). \quad (11)$$

The cross section for neutrino capture to a specific state, j , in ^{205}Pb is given by

$$\sigma_j(E_{\nu_e}) = \frac{2\pi^2 \hbar^3 \ln(2)}{\mathcal{K} m_e^5 c^7} p_e E_e F(Z, E_e) C_j(E_{\nu_e}), \quad (12)$$

where $E_e = E_{\nu_e} - \Delta Mc^2 - E_j^* + m_e c^2$ is the total energy of the emitted electron, $\Delta Mc^2 = 50.6(5)$ keV is the atomic mass difference, E_j^* is the excitation energy of the final ^{205}Pb j state, p_e is the momentum of the emitted electron, $F(Z, E_e)$ is the Fermi function, which we evaluate following the analytical approximation from [15], and $\mathcal{K} = 2\mathcal{F}t = 6144.5(37)$ s is the corrected β -decay constant that includes the independent radiative correction Δ_R^V as detailed in [16].

Individual neutrino rates—To obtain the neutrino capture rate, we integrate over the neutrino flux $\Phi_i(E_{\nu_e})$ accounting for each individual contribution i to the flux.

Then the neutrino capture rate R_i in solar neutrino units (SNU) for a given neutrino flux is given by

$$R_i = 10^{36} \times \sum_j \int \sigma_j(E_{\nu_e}) \Phi_i(E_{\nu_e}) dE_{\nu_e} \quad [\text{SNU}]. \quad (13)$$

We use solar neutrino fluxes from the global analysis of solar neutrino data including the final results of the three phases of BOREXINO (Eq. (3.3) of [17])¹. We adopted the neutrino spectrum shape available on J. N. Bahcall's website [18] for all the solar-neutrino fluxes, except for ⁸B, for which we use the accurate determination by Longfellow *et al.* [19].

To account for the oscillation of the solar neutrinos, we adopted the solar neutrino survival probability factors extracted from Fig. 14.3 of [20], as provided by the Particle Data Group Collaboration. We show in Table I the neutrino survival factors together with the contributions of individual neutrino fluxes to the solar neutrino capture rate on ²⁰⁵Tl expressed in SNU *without* considering neutrino oscillations. Furthermore, the contributions of the ⁸B and *hep* neutrino fluxes are split into two parts. On the one hand, we have the contribution mediated by first-forbidden operators to states of ²⁰⁵Pb with $I^\pi = 1/2^-, 3/2^-, \text{ and } 5/2^-$. On the other hand, as discussed above, we have evaluated the contribution mediated by the Gamow-Teller operator to states of ²⁰⁵Pb with $I^\pi = 1/2^+ \text{ and } 3/2^+$ based on data from the ²⁰⁵Tl(*p,n*)²⁰⁵Pb reaction [14]. As there are no $1/2^+$ or $3/2^+$ states known below 2.75 MeV and as the measured strength for these low energies is compatible with zero, we only consider the possibility of neutrino capture mediated by GT to ²⁰⁵Pb states with an excitation energy > 2.75 MeV.

* ragan.sidhu@ed.ac.uk

† r.chen@gsi.de

‡ riccardo.mancino@matfyz.cuni.cz; Present address: Faculty of Mathematics and Physics, Charles University, Prague, Czech Republic

§ Deceased

- [1] C. Trageser, C. Brandau, C. Kozhuharov, Y. A. Litvinov, A. Müller, F. Nolden, S. Sanjari, and T. Stöhlker, *Phys. Scr.* **2015**, 014062 (2015).
- [2] C. Trageser, *PhD Thesis, Justus-Liebig-Universität* (2018).
- [3] R. S. Sidhu, *PhD Thesis, Ruprecht-Karls-Universität* (2021).
- [4] G. Leckenby, R. S. Sidhu, R. J. Chen, Y. Litvinov, J. Glorius, C. Griffin, and I. Dillmann (E121 Collaboration), *EPJ Web Conf.* **279**, 06010 (2023).
- [5] M. Jung, F. Bosch, K. Beckert, H. Eickhoff, H. Folger, B. Franzke, A. Gruber, P. Kienle, O. Klepper, W. Koenig, *et al.*, *Phys. Rev. Lett.* **69**, 2164 (1992).
- [6] F. Bosch, T. Faestermann, J. Friese, F. Heine, P. Kienle, E. Wefers, K. Zeitelhack, K. Beckert, B. Franzke, O. Klepper, *et al.*, *Phys. Rev. Lett.* **77**, 5190 (1996).
- [7] D. J. Millener, D. E. Alburger, E. K. Warburton, and D. H. Wilkinson, *Phys. Rev. C* **26**, 1167 (1982).
- [8] H. Behrens and W. Bühring, *Electron radial wave functions and nuclear beta decay* (Clarendon, Oxford, 1982).
- [9] Q. Zhi, E. Caurier, J. J. Cuenca-García, K. Langanke, G. Martínez-Pinedo, and K. Sieja, *Phys. Rev. C* **87**, 025803 (2013).
- [10] W. Bambynek, H. Behrens, M. H. Chen, B. Crasemann, M. L. Fitzpatrick, K. W. D. Ledingham, H. Genz, M. Mutterer, and R. L. Intemann, *Rev. Mod. Phys.* **49**, 77 (1977).
- [11] E. Caurier, G. Martínez-Pinedo, F. Nowacki, A. Poves, and A. P. Zuker, *Rev. Mod. Phys.* **77**, 427 (2005).
- [12] E. K. Warburton, *Phys. Rev. C* **44**, 233 (1991).
- [13] R. Mancino, T. Neff, and G. Martínez-Pinedo, (to be published).
- [14] D. Krofcheck, *PhD Thesis, Ohio State University* (1987).
- [15] G. K. Schenter and P. Vogel, *Nucl. Sci. and Eng.* **83**, 393 (1983).
- [16] J. C. Hardy and I. S. Towner, *Phys. Rev. C* **102**, 045501 (2020).
- [17] M. C. Gonzalez-Garcia, M. Maltoni, J. P. Pinheiro, and A. M. Serenelli, *J. of High Energy Phys.* **2024**, 64 (2024).
- [18] J. N. Bahcall, *Software and data for solar neutrino research* (2005).
- [19] B. Longfellow, A. T. Gallant, T. Y. Hirsh, M. T. Burkey, G. Savard, N. D. Scielzo, L. Varriano, M. Brodeur, D. P. Burdette, J. A. Clark, D. Lascar, P. Mueller, D. Ray, K. S. Sharma, A. A. Valverde, G. L. Wilson, and X. L. Yan, *Phys. Rev. C* **107**, L032801 (2023).
- [20] S. Navas, C. Amsler, T. Gutsche, C. Hanhart, J. J. Hernández-Rey, C. Lourenço, A. Masoni, M. Mikhasenko, R. E. Mitchell, C. Patrignani, *et al.* (Particle Data Group Collaboration), *Phys. Rev. D* **110**, 030001 (2024).

¹ We have corrected a typo in the ¹⁷F flux provided in [17]. It should be $5.51^{+0.75}_{-0.63} \times 10^6 \text{ cm}^{-2} \text{ s}^{-1}$ instead of $5.51^{+0.75}_{-0.63} \times 10^7 \text{ cm}^{-2} \text{ s}^{-1}$.